Supplementary Materials for

Spatiotemporal Brain Transcriptomics Reveal Risk Gene Hot-Spots in Major Neuropsychiatric Disorders

Weiqing Liu[1*], Tomomi Shimogori[2*]

[1]Clinical Research Center for Mental Disorders, Shanghai Pudong New Area Mental Health Center, School of Medicine, Tongji University, 165 Sanlin Road, Pudong New Area, Shanghai 200124, China
[2]Laboratory for Molecular Mechanisms of Brain Development, Center for Brain Science, RIKEN, 2-1 Hirosawa, Wako, Saitama 351-0198, Japan

* These authors jointly supervised this work
Weiqing Liu, Email: liuwq2010@tongji.edu.cn
Tomomi Shimogori, Email: tomomi.shimogori@riken.jp

This file includes:

Supplementary Figures 1-19

Supplementary Table 1

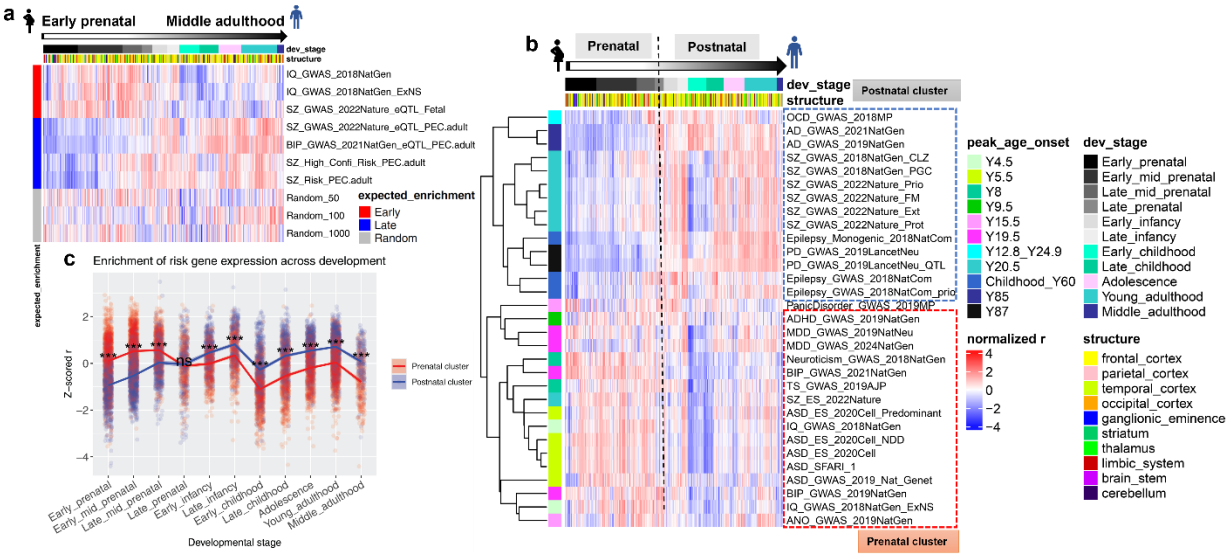

Supplementary Figure 1. Validation and developmental stratification of spatiotemporal expression enrichment patterns of neuropsychiatric risk gene sets

(a) Positive and negative control gene sets exhibited the expected spatiotemporal expression enrichment patterns. Risk gene sets derived from IQ GWAS and fetal brain eQTL–associated genes showed prominent prenatal enrichment (early-enriched controls), whereas gene sets based on adult brain eQTLs and the PsychENCODE Phase I integrative analysis—predominantly derived from adult transcriptomes—displayed peak enrichment during postnatal stages (late-enriched controls). In contrast, randomly generated gene sets used as negative controls showed no consistent spatial or temporal enrichment patterns. Red and blue color gradients represent Z-scored rank biserial correlation coefficients from Mann–Whitney U tests, indicating relative enrichment or depletion of gene set expression across BrainSpan samples. Colored labels and annotations indicate developmental stages, brain structures, and control gene set identities.

(b) Hierarchical clustering of developmental enrichment trajectories across neuropsychiatric risk gene sets revealed a clear separation between prenatally and postnatally enriched disorder groups. Risk gene sets derived from the same disorder clustered closely together, indicating strong internal consistency across datasets. Prenatally and postnatally enriched disorder groups are highlighted by red and blue dashed boxes, respectively. Colored labels and annotations denote developmental stages, brain structures and the peak age of onset for each disorder.

(c) Line plots comparing the developmental dynamics of risk gene expression enrichment between the prenatally and postnatally overrepresented disorder clusters. For each developmental stage, lines represent the mean Z-scored *r* value across datasets within each cluster. Shaded ribbons indicate the 95% confidence interval of the mean (mean ± 1.96 × SE). Individual data points show standardized enrichment values for individual sample and are displayed with horizontal jitter to illustrate the underlying data distribution. The two trajectories intersect during late prenatal development, marking a transitional phase between prenatal and postnatal dominance. Statistical differences between the two clusters at each developmental stage were assessed using Wilcoxon rank-sum tests, with

false discovery rate (FDR)–corrected *P* values indicated above the curves (FDR-adjusted $P > 0.05$ and $P < 0.001$ denoted by “ns” and ***, respectively).
GWAS, Genome-Wide Association Studies; ES, Exome Sequencing; ExNS, Exonic non-synonymous variants; eQTL, expression Quantitative Trait Loci; PEC, PsychEnCode; NDD, Neurodevelopmental disorders; PGC, Psychiatric Genomics Consortium; CLOZUK, Clozapine-treated schizophrenia cohort from the United Kingdom; Ext, Extended GWAS; Prot, Portein Coding; Prio, Prioritized; FM, Fine mapping; IQ, Intelligence Quotient; ASD, Autism Spectrum Disorders; ADHD, Attention Deficit Hyperactive Disorder; TS, Tourette's Syndrome; OCD, Obsessive Compulsive Disorder; ANO, Anorexia Nervosa; MDD, Major Depressive Disorder; BIP, Bipolar Disorder; SZes, Schizophrenia exome sequencing; SZgw, Schizophrenia gwas; AD, Alzheimer's Disease; PD, Parkinson's Disease.

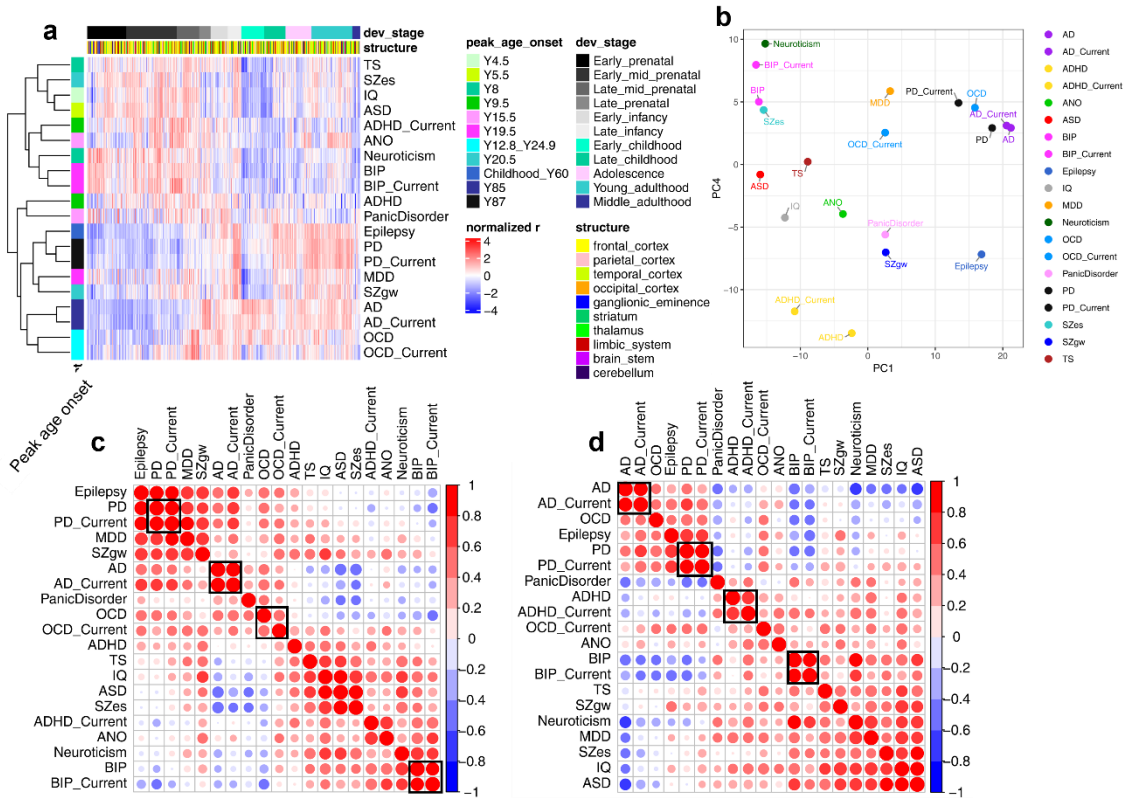

Supplementary Figure 2. Validation of the spatiotemporal enrichment and clustering patterns with the most current published GWAS datasets.

(a) Spatiotemporal expression enrichment heatmap including the original 15 risk gene datasets together with five additional recently published GWAS datasets for ADHD, BIP, OCD, AD, and PD. Hierarchical clustering based on enrichment patterns revealed that approximately 80% of the newly added risk gene sets clustered in close proximity to their corresponding original datasets, supporting the robustness of the spatiotemporal enrichment and clustering structure. Notably, the newly added ADHD-current dataset occupied the position previously associated with ADHD, whereas the original ADHD dataset clustered closer to panic disorder, lying between the prenatally and postnatally enriched groups. This shift suggests that limited sample size in the ADHD risk gene datasets may contribute to instability in spatiotemporal enrichment patterns.

(b) Principal component analysis (PCA) was performed on the Z-scored rank biserial correlation coefficients of the initial 15 risk gene sets together with five additional recently published GWAS datasets for ADHD, BIP, OCD, AD and PD. The scatter plot shows the distribution of the five additional datasets are consistent with the initial positions for the same trait in the space defined by the temporal (PC1) and spatial (PC4) principal components.

(c-d) Correlation matrices illustrate the relationships among the initial 15 traits together with five additional recently published GWAS datasets for ADHD, BIP, OCD, AD and PD based on enrichment patterns in cortical samples (c) and subcortical samples (d). Four out of the five datasets pairs for the same traits are highly correlated with each other in both the cortical and subcortical samples, as indicated by black boxes respectively in panel c and d.

IQ, Intelligence Quotient; ASD, Autism Spectrum Disorders; ADHD, Attention Deficit Hyperactive Disorder; TS, Tourette's Syndrome; OCD, Obsessive Compulsive Disorder; ANO, Anorexia Nervosa; MDD, Major Depressive Disorder; BIP, Bipolar Disorder; SZes, Schizophrenia exome sequencing; SZgw, Schizophrenia gwas; AD, Alzheimer's Disease; PD, Parkinson's Disease.

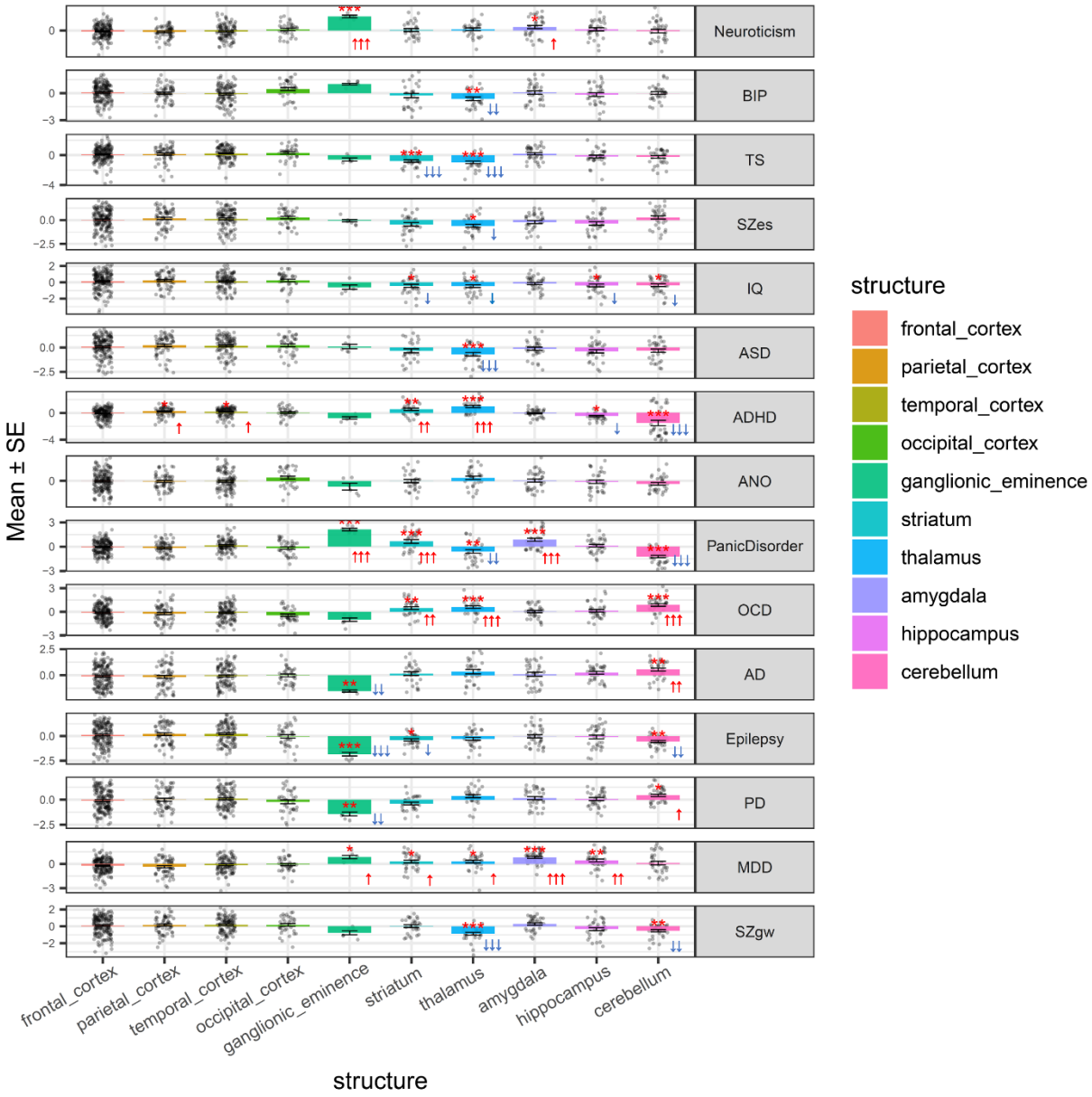

Supplementary Figure 3. Comparison of risk gene expression enrichment across major brain regions.

Bar plots with individual sample points illustrate the relative enrichment of risk gene set expression across major brain structures. The frontal cortex was used as the reference structure due to its largest sample size in the BrainSpan dataset and its well-established relevance in cognition and psychiatric disorders. For each of the 15 traits, enrichment levels in all other structures were compared with those in the frontal cortex using t-tests. Sample sizes were as follows: frontal cortex (n = 164), parietal cortex (n = 61), temporal cortex (n = 102), occipital cortex (n = 35), ganglionic eminence (n = 6), striatum (n = 28), thalamus (n = 29), amygdala (n = 33), hippocampus (n = 32), and cerebellum (n = 32). The brainstem was excluded from these comparisons due to its small sample size (n<5). Data are presented as mean ± standard error of the mean (SEM). FDR-corrected P values < 0.05, 0.01, or 0.001 are indicated by one, two, or three asterisks respectively. To facilitate visualization of the comparison results, red arrows denote significantly higher enrichment

relative to the frontal cortex, whereas blue arrows denote significantly lower enrichment. The number of arrows corresponds to the significance level (P_{FDR} < 0.05, 0.01, or 0.001 were denoted by one, two or three arrows, respectively).

IQ, Intelligence Quotient; ASD, Autism Spectrum Disorders; ADHD, Attention Deficit Hyperactive Disorder; TS, Tourette's Syndrome; OCD, Obsessive Compulsive Disorder; ANO, Anorexia Nervosa; MDD, Major Depressive Disorder; BIP, Bipolar Disorder; SZes, Schizophrenia exome sequencing; SZgw, Schizophrenia gwas; AD, Alzheimer's Disease; PD, Parkinson's Disease.

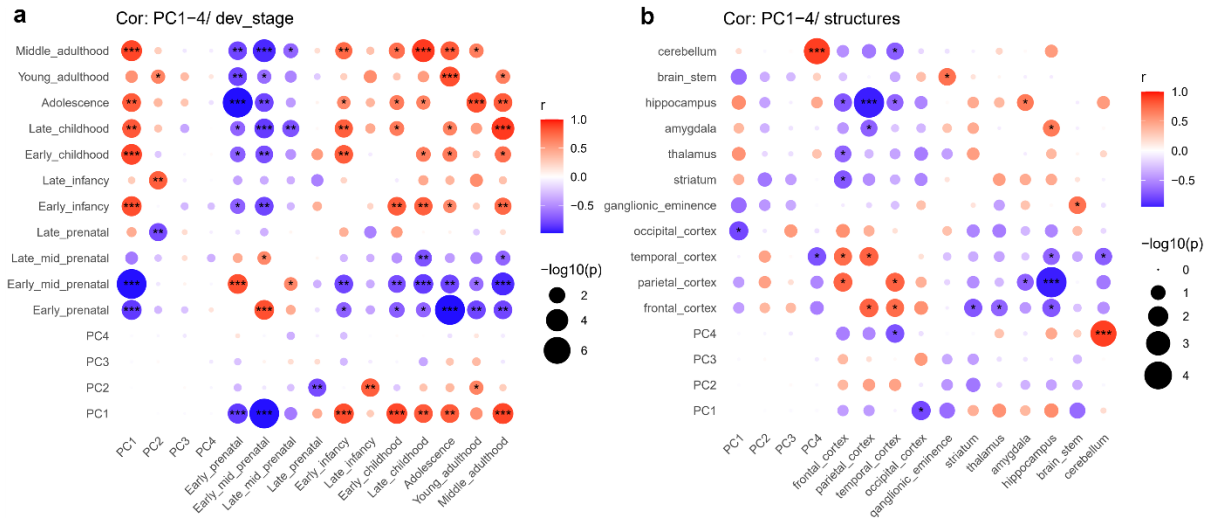

Supplementary Figure 4. Correlation matrix between the PCA components and individual spatiotemporal enrichment variables across 15 neuropsychiatric traits.

(a) Bubble heatmaps showing pairwise correlations between PCA-derived components (PC1-PC4) and the mean enrichment values of risk gene sets across developmental stages. Each cell displays the Spearman correlation coefficient (*r*) between PC scores and enrichment values across developmental stages, with colors indicating the direction and magnitude of the correlation. Bubble size represents -log10(*P*), and asterisks denote FDR-corrected significance (P_{FDR} < 0.05: *; P_{FDR} < 0.01: **; P_{FDR} < 0.001: ***). Notably, PC1 shows a clear monotonic shift in association from prenatal to postnatal samples, while PC2 shows significant associations with risk gene enrichment during late infancy and young adulthood. Overall, prenatal- and postnatal- developmental stages display opposing enrichment dynamics.

(b) A similar bubble heatmap illustrating correlations between PC1–PC4 and structure-specific enrichment variables. PC4 shows a significant positive association with risk gene enrichment in the cerebellum, whereas PC1 is negatively associated with enrichment in the occipital cortex. Consistent with panel (a), cortical and subcortical regions exhibit distinct patterns of risk gene enrichment.

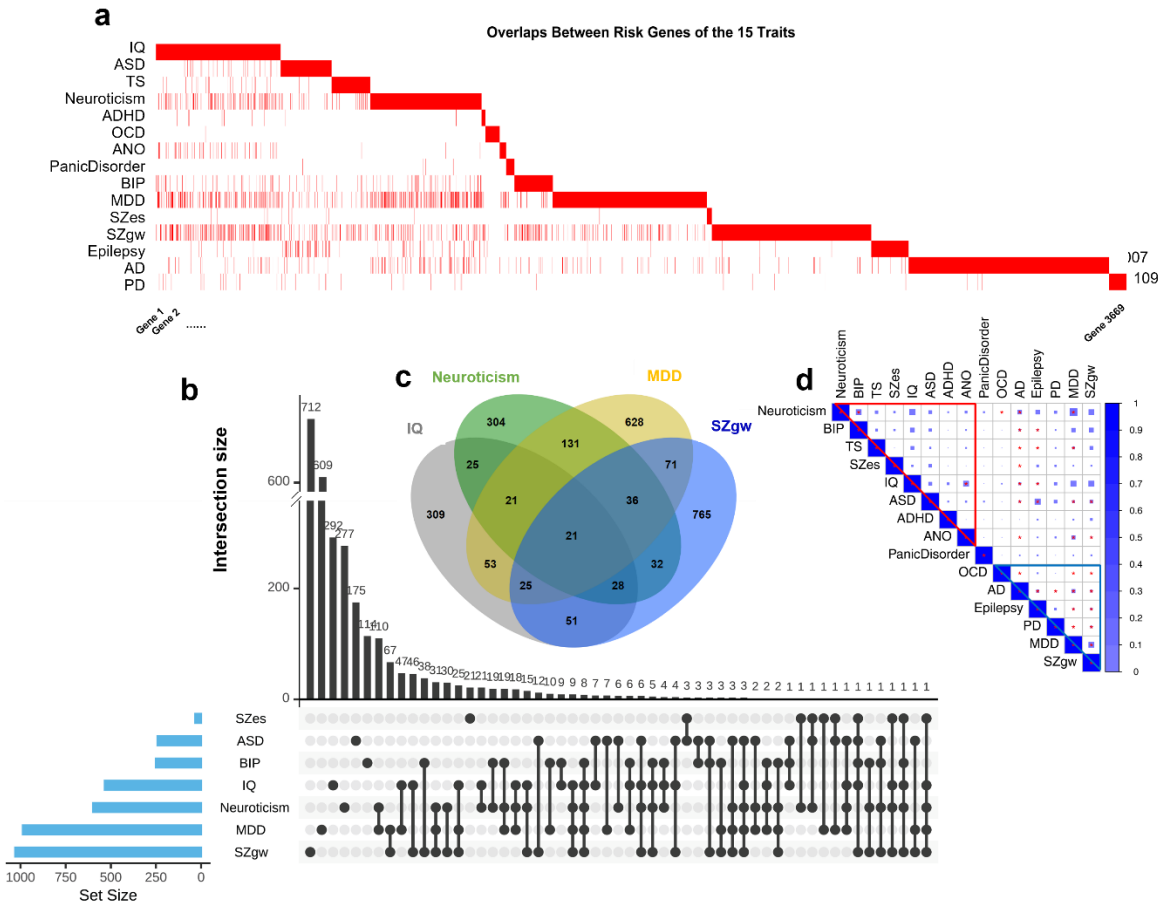

Supplementary Figure 5. Similarities between risk gene sets do not account for the spatiotemporal clustering of the 15 traits.

(a) Sizes of the 15 risk gene sets for major neuropsychiatric disorders and their gene overlaps. Each row represents a trait risk gene set, with the total number of genes indicated at the end of the row. Columns correspond to all 3,669 unique genes across the 15 sets; red cells in each row denote composition risk genes for the traits.

(b) UpSet plot illustrating gene overlaps among traits. Notably, traits assigned to the same cluster (e.g., SZes, IQ, and ASD in the “Prenatal cortical” cluster; MDD and BIP in the “Prenatal subcortical” cluster) exhibited limited gene overlap, indicating that the t-SNE-based clustering was driven by similarities in spatiotemporal expression profiles rather than gene set overlap.

(c) Overlaps among major neuropsychiatric disorder risk gene sets.

(d) Pairwise Jaccard similarity analysis among the 15 gene sets. Traits are ordered by their corresponding clusters. Intra-cluster correlations are indicated by triangles, while inter-cluster correlations are shown outside the triangles. Square sizes reflect Jaccard similarity coefficients; asterisks denote statistical significance (P<0.05/120). Overall, pairwise similarities were low, with the highest observed between MDD and neuroticism (J = 0.15). Importantly, most traits within the same cluster showed generally lower similarities with each other than that with traits from different clusters. For example, IQ, ASD, TS, and SZes in the “Prenatal” cluster, and SZgw, AD, PD, and epilepsy in the “Postnatal” cluster, all

exhibited lower pairwise similarities, supporting the conclusion that the observed clustering of traits reflects shared spatiotemporal expression patterns rather than overlapping gene content.

IQ, Intelligence Quotient; ASD, Autism Spectrum Disorders; ADHD, Attention Deficit Hyperactive Disorder; TS, Tourette's Syndrome; OCD, Obsessive Compulsive Disorder; ANO, Anorexia Nervosa; MDD, Major Depressive Disorder; BIP, Bipolar Disorder; SZes, Schizophrenia exome sequencing; SZgw, Schizophrenia gwas; AD, Alzheimer's Disease; PD, Parkinson's Disease.

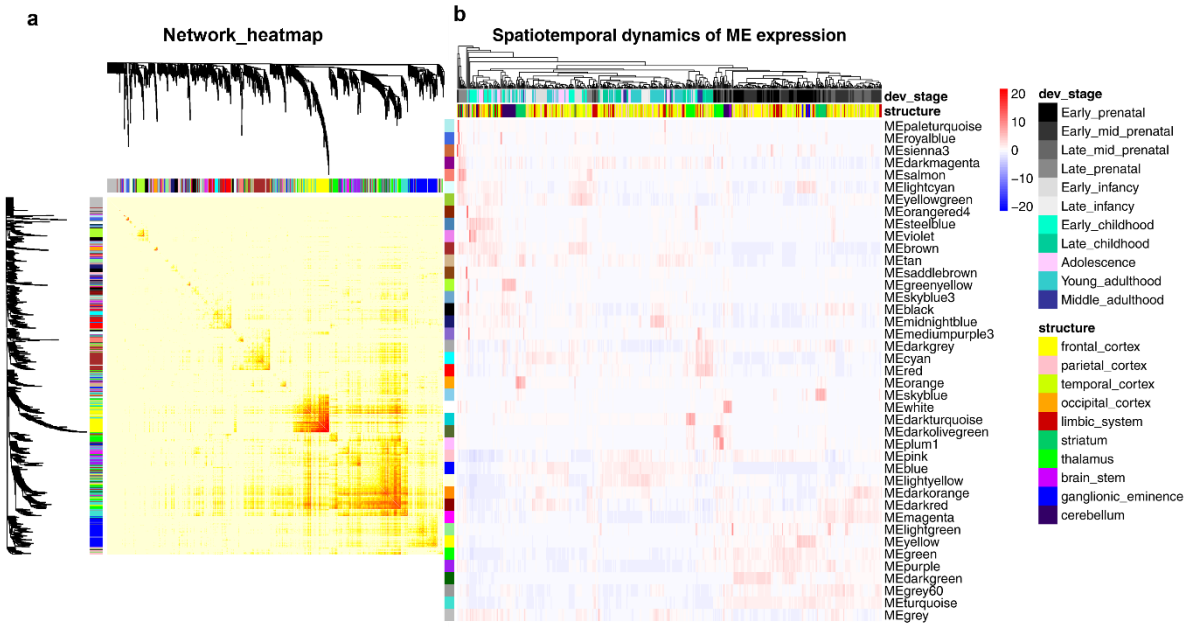

Supplementary Figure 6. WGCNA based spatiotemporal co-expression modules

WGCNA was applied on the BrainSpan transcriptomic dataset to identify modules of co-expressed genes across developmental stages and brain regions. A total of 41 co-expression modules were initially identified.

(a) Network heatmap visualizes the TOM-based dissimilarity among 400 randomly selected genes. The dissimilarity matrix (1 − TOM) was raised to the 7th power to enhance contrast, and hierarchical clustering was applied to organize the genes. Each gene is colored according to its assigned co-expression module, facilitating the identification of distinct module structures and network connectivity patterns.

(b) Spatiotemporal dynamics of module eigengene (ME) expression. Heatmap of the expression levels of 41 MEs across 521 BrianSpan transcriptomes, spanning 11 developmental stages and 10 major brain structures. Expression values are row-scaled for each ME, with hierarchical clustering performed on the samples. Sample annotations are color-coded by developmental stage and brain region, highlighting dynamic and region-specific co-expression module activity across human brain development. The heatmap illustrated significant enrichment of module genes expression in a spatiotemporal specific pattern.

WGCNA, Weighted Gene Co-expression Network Analysis; TOM, topological overlap matrix; ME, module eigengene.

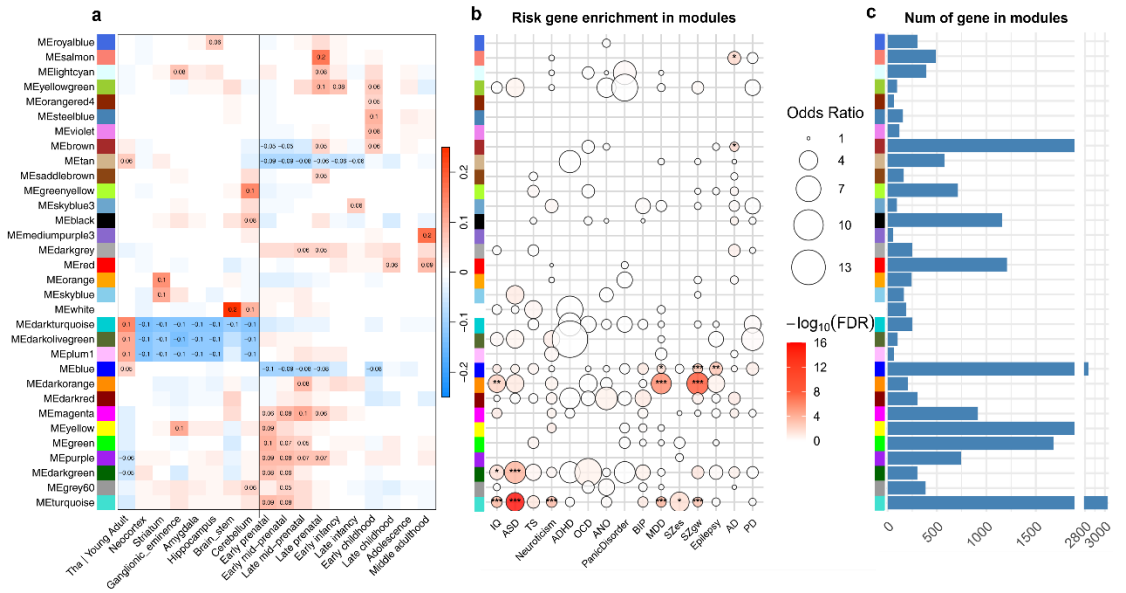

Supplementary Figure 7. Module eigengene (minModuleSize=40) enrichment in spatiotemporal levels and risk gene sets.

(a) Linear regression models were used to assess the influence of brain region and developmental stage (encoded as dummy variables) on ME expression levels. The thalamus during young adulthood was set as the reference category and absorbed into the model intercept, which thus represents the baseline expression of each module. Predicted ME expression levels for other regions and developmental stages were computed by adding corresponding *B* coefficients to the intercept, allowing identification of spatiotemporal expression peaks ("hot-spots") for each module. Only 32 modules that showed the most significant spatial or temporal expression enrichment (with at least one $B > 0.05$ in the regression model) were retained for visualization in the heatmap. Within these modules, only module–spatiotemporal variable level combinations with an absolute regression coefficient $|B| \geq 0.05$ and a false discovery rate (FDR)–corrected *P* value < 0.05 are displayed,, with red colors indicate enrichment of module gene expression and blue indicate deprivation. Modules on the y-axis are ordered according to their eigengene similarity distance derived from WGCNA hierarchical clustering.

(b) Enrichment of neuropsychiatric disorder risk gene sets across the 32 spatiotemporal modules. Odds ratios (ORs) and *P* values from chi-square tests are displayed in the Trait × Module matrix, with the size of bubbles indicating OR values and color gradient indicating $-\log_{10}$ (FDR) magnitude. Notably, the ADHD × MEdarkolivegreen combination showed the highest OR (14), though the P_{FDR} value was not significant, likely reflecting the limited size of the ADHD risk gene set. *P* values across all the 41 WGCNA detected modules for each of the disorders were FDR corrected ($P_{FDR} < 0.05$: *; $P_{FDR} < 0.01$: **; $P_{FDR} < 0.001$: ***)..

(c) Horizontal bar plot showing the number of genes in each of the 32 co-expression modules. Due to the substantial variability in module size (ranging from 56 to 3030 genes), the x-axis was truncated between 1800-2800 using a broken scale to improve visualization of both small and large modules. This visualization highlights the pronounced imbalance

in module sizes, which may influence downstream enrichment analyses, as larger modules tend to yield stronger statistical significance, whereas smaller modules may exhibit higher odds ratios but reduced statistical power.

WGCNA, Weighted Gene Co-expression Network Analysis; ME, module eigengene; Tha, Thalamus; IQ, Intelligence Quotient; ASD, Autism Spectrum Disorders; ADHD, Attention Deficit Hyperactive Disorder; TS, Tourette's Syndrome; OCD, Obsessive Compulsive Disorder; ANO, Anorexia Nervosa; MDD, Major Depressive Disorder; BIP, Bipolar Disorder; SZes, Schizophrenia exome sequencing; SZgw, Schizophrenia gwas; AD, Alzheimer's Disease; PD, Parkinson's Disease.

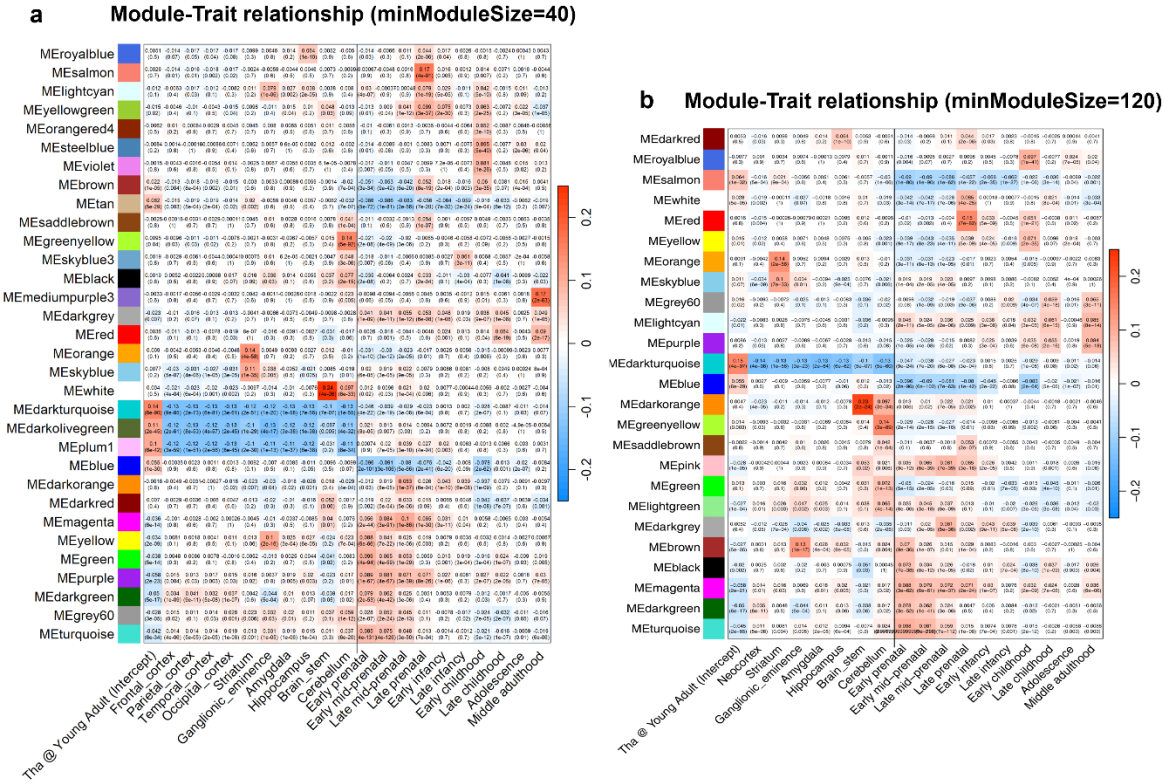

Supplementary Figure 8. Module identification under different minimum module size settings.

(a, b) WGCNA results obtained using different minimum module size thresholds, with a minimum module size of 40 in panel a and 120 in panel b. In both panels, only modules whose module eigengenes (MEs) exhibited at least one regression coefficient (*B*) ≥ 0.05 for any spatial or temporal variable level are shown. Modules on the y-axis are ordered according to their eigengene similarity distance derived from WGCNA hierarchical clustering. Overall, a high degree of similarity was observed between the two analyses. Several modules with spatiotemporally specific expression patterns were consistently identified under both parameter settings, exhibiting highly comparable enrichment profiles across developmental stages and brain regions. These modules likely represent corresponding co-expression module pairs detected under different minimum size constraints. Representative paired modules include turquoise–turquoise, darkgreen–darkgreen, yellow–brown, brown-yellow, purple–magenta, darkturquoise–darkturquoise, blue–blue, orange–orange, greenyellow–greenyellow, white–darkorange, royalblue–darkred, and salmon–red (panel a–panel b, respectively).

Tha, Thalamus; ME, module eigengene;

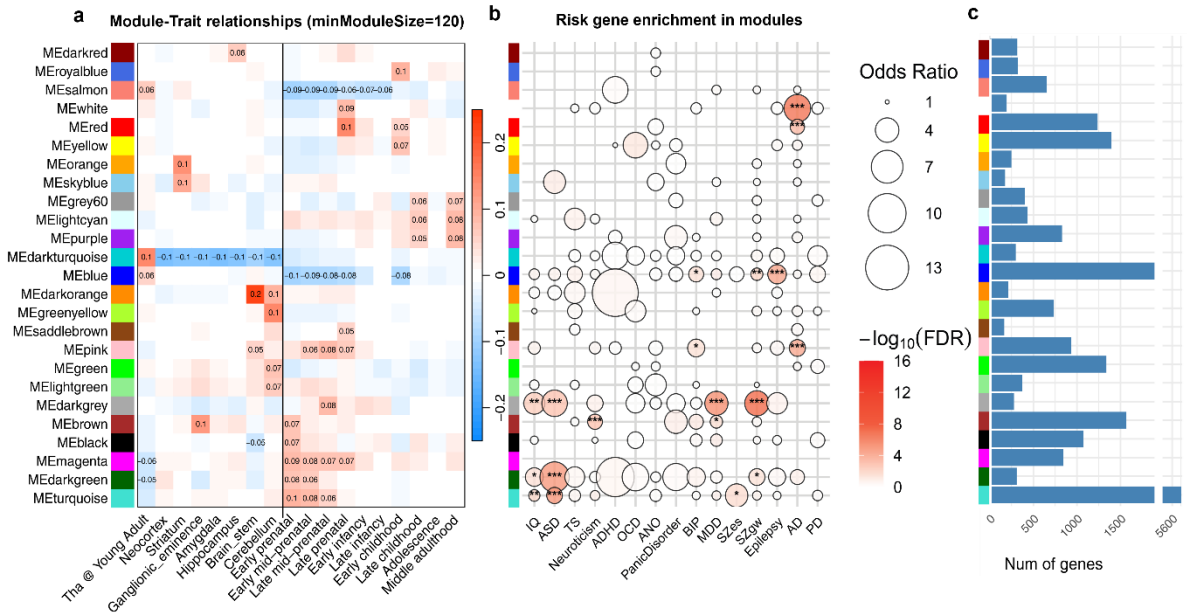

Supplementary Figure 9. Module eigengene (min size=120) enrichment in spatiotemporal levels and risk gene sets.

(a) Linear regression models were used to assess the influence of brain region and developmental stage (encoded as dummy variables) on ME expression levels, when the minimum size was set as 120. The thalamus during young adulthood was set as the reference category and absorbed into the model intercept, which thus represents the baseline expression of each module. Predicted ME expression levels for other regions and developmental stages were computed by adding corresponding *B* coefficients to the intercept, allowing identification of spatiotemporal expression peaks ("hot-spots") for each module. Only 25 modules that showed the most significant spatial or temporal expression enrichment (with at least one $B > 0.05$ in the regression model) were retained for visualization in the heatmap. Within these modules, only module–spatiotemporal variable level combinations with an absolute regression coefficient $|B| \geq 0.05$ and a false discovery rate (FDR)–corrected *P* value < 0.05 are displayed, with red colors indicate enrichment of module gene expression and blue indicate deprivation. Modules on the y-axis are ordered according to their eigengene similarity distance derived from WGCNA hierarchical clustering.

(b) Enrichment of neuropsychiatric disorder risk gene sets across the 25 spatiotemporal modules. Odds ratios (ORs) that higher than 1 and the corresponding *P* values from chi-square tests are displayed in the Trait × Module matrix, with the size of bubbles indicating OR values and color gradient indicating $-\log_{10}$ (FDR) magnitude. *P* values across all the original 31 WGCNA detected modules for each of the disorders were FDR corrected ($P_{FDR} < 0.05$: *; $P_{FDR} < 0.01$: **; $P_{FDR} < 0.001$: ***).

(c) Horizontal bar plot showing the number of genes in each of the 25 co-expression modules. Due to the substantial variability in module size (ranging from 166 to 5705 genes), the x-axis was truncated between 1800-5500 using a broken scale to improve visualization of both small and large modules.

ME, module eigengene; Tha, Thalamus; IQ, Intelligence Quotient; ASD, Autism Spectrum Disorders; ADHD, Attention Deficit Hyperactive Disorder; TS, Tourette's Syndrome; OCD, Obsessive Compulsive Disorder; ANO, Anorexia Nervosa; MDD, Major Depressive Disorder; BIP, Bipolar Disorder; SZes, Schizophrenia exome sequencing; SZgw, Schizophrenia gwas; AD, Alzheimer's Disease; PD, Parkinson's Disease.

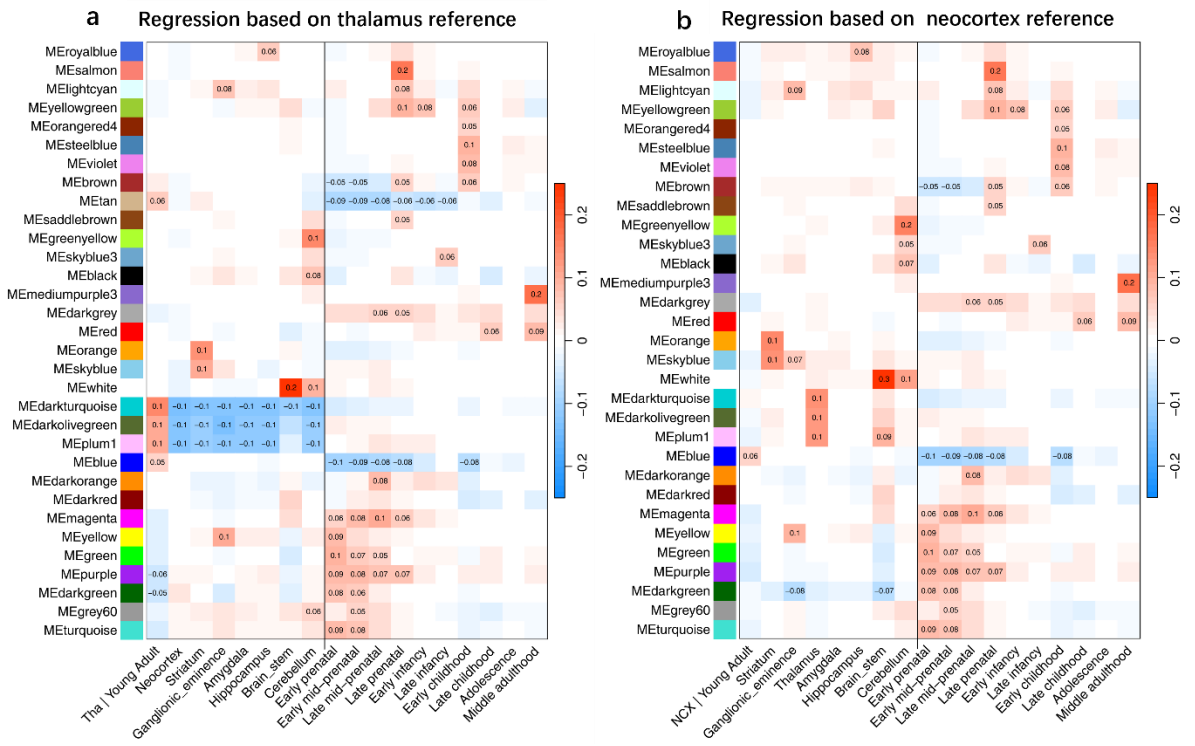

Supplementary Figure 10. Comparison of spatiotemporal ME enrichment patterns under different dummy-variable reference levels.

Heatmaps showing spatiotemporal enrichment patterns of module eigengenes (MEs) derived from linear regression models using different reference brain regions, with thalamus at young adulthood as the reference in panel (a) and neocortex at young adulthood as the reference in panel (b). In both panels, only modules exhibiting at least one regression coefficient (B) $\geqslant$0.05 are displayed, and only the regression coefficients for spatial or temporal variable levels with an $|B| \geqslant 0.05$ and a $P_{FDR} < 0.05$ are shown. Although the absolute ME expression levels of the reference brain regions differ between the two models, the relative expression differences of each ME across brain regions and developmental stages are highly consistent. This concordance indicates that the choice of reference level affects the intercept and parameter interpretation but does not alter the identification of spatiotemporal enrichment patterns.

ME, module eigengene; Tha, Thalamus; NCX, Neocortex.

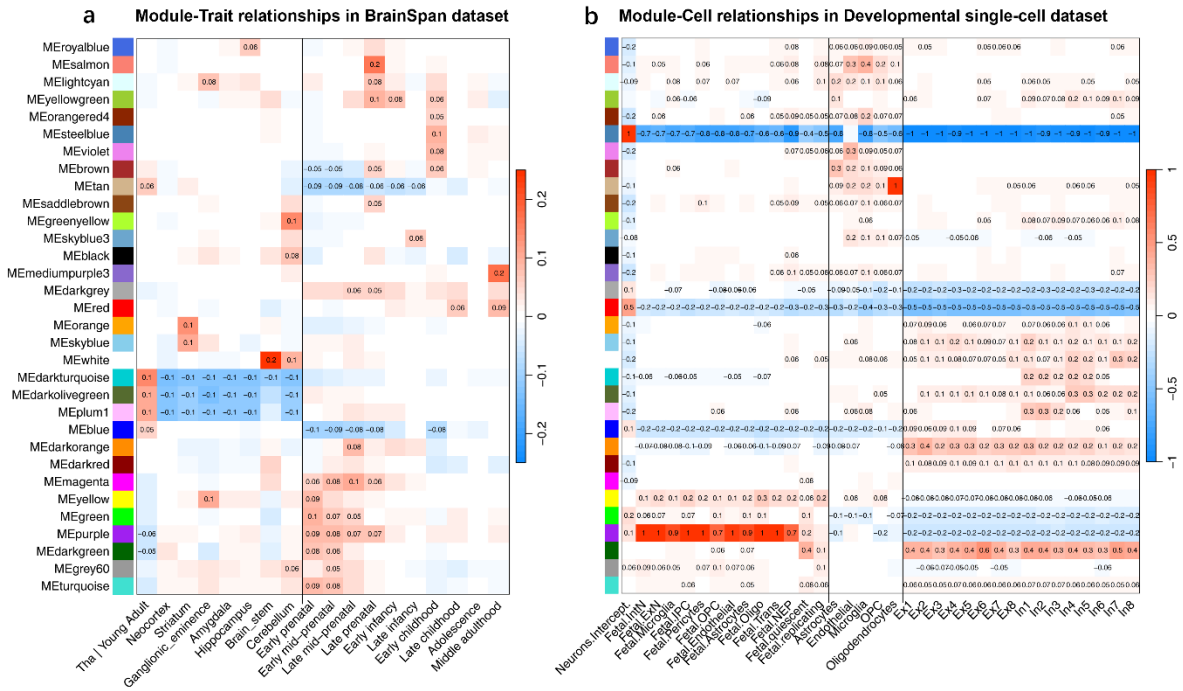

Supplementary Figure 11. Parallel comparison of module – spatiotemporal and module–cell-type associations.

(a) Spatiotemporal enrichment patterns of module eigengenes (MEs), reproduced from Fig. S7a for direct comparison. Linear regression models were used to evaluate the effects of brain region and developmental stage (encoded as dummy variables) on ME expression levels, with the thalamus during young adulthood set as the reference category and absorbed into the model intercept.

(b) Cell-type–specific enrichment of the same modules. Linear regression models were used to assess the influence of major brain cell types (encoded as dummy variables) on ME expression levels. Adult neurons were used as the reference category and absorbed into the model intercept, representing baseline module expression. Predicted ME expression levels for other cell types were obtained by adding the corresponding regression coefficients (B) to the intercept. Only the 32 modules that showed the most significant spatial or temporal enrichment in panel (a) were retained for visualization in both panels. Heatmaps display only module–cell-type combinations with an absolute regression coefficient $|B| \geq 0.05$ and a $P_{FDR} < 0.05$. Red indicates relative enrichment of module gene expression, whereas blue indicates relative depletion. Modules on the y-axis are ordered according to eigengene similarity distances derived from WGCNA hierarchical clustering.

ME, module eigengene; IntN, Inhibitory Neurons; ExN, Excitatory Neurons; IPC, Intermediate Progenitor Cells; OPC, Oligodendrocyte Precursor Cells; Oligo, Oligodendrocytes; Tans, Transitioning cells; NEP, Neural Epithelial Progenitors; Excitatory neurons; In, Inhibitory neurons.

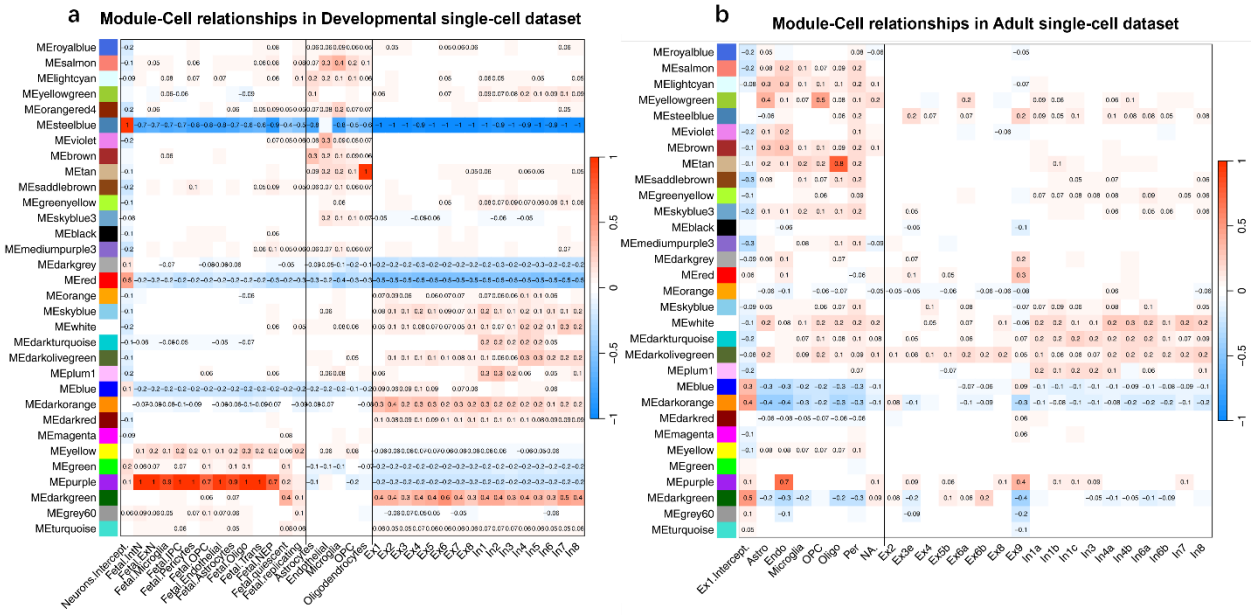

Supplementary Figure 12. Module–Cell type relationships in developmental and adult single-cell transcriptomic datasets.

(a) Module – Cell type associations derived from the developmental single-cell transcriptomic dataset, with adult neurons specified as the reference category in the regression model.

(b) Module–Cell type associations derived from the adult single-cell transcriptomic dataset, with excitatory neuron subtype Ex1 specified as the reference category.

In both panels, only modules exhibiting at least one regression coefficient (B) $\geqslant$ 0.05 are shown. Within these modules, only module–cell type combinations with an absolute regression coefficient $|B| \geqslant 0.05$ and a $P_{FDR} < 0.05$ are displayed. Accordingly, all B values shown in the heatmaps represent statistically significant associations.

Despite differences in dataset composition and reference cell types, modules enriched in glial cell types in the developmental dataset (e.g., MEsalmon, MElightcyan, MEyellowgreen, MEviolet, MEbrown, and MEtan) exhibit concordant enrichment in corresponding glial populations in the adult dataset, indicating robust and conserved module – cell type expression patterns across developmental stages. Likewise, modules preferentially expressed in interneurons in the developmental dataset (e.g., MEwhite, MEdarkturquoise, and MEplum1) display concordant enrichment in interneuron populations in the adult dataset. This cross-dataset concordance argues against dataset-dependent artifacts and supports the interpretation that these modules represent cell-type–specific and functionally specialized gene co-expression programs.

ME, module eigengene; IntN, Inhibitory Neurons; ExN, Excitatory Neurons; IPC, Intermediate Progenitor Cells; OPC, Oligodendrocyte Precursor Cells; Oligo, Oligodendrocytes; Tans, Transitioning cells; NEP, Neural Epithelial Progenitors; Ex, Excitatory neurons; In, Inhibitory neurons; Astro, Astrocytes; Endo, Endothelial cells; Per, Pericytes; NA, Not Available.

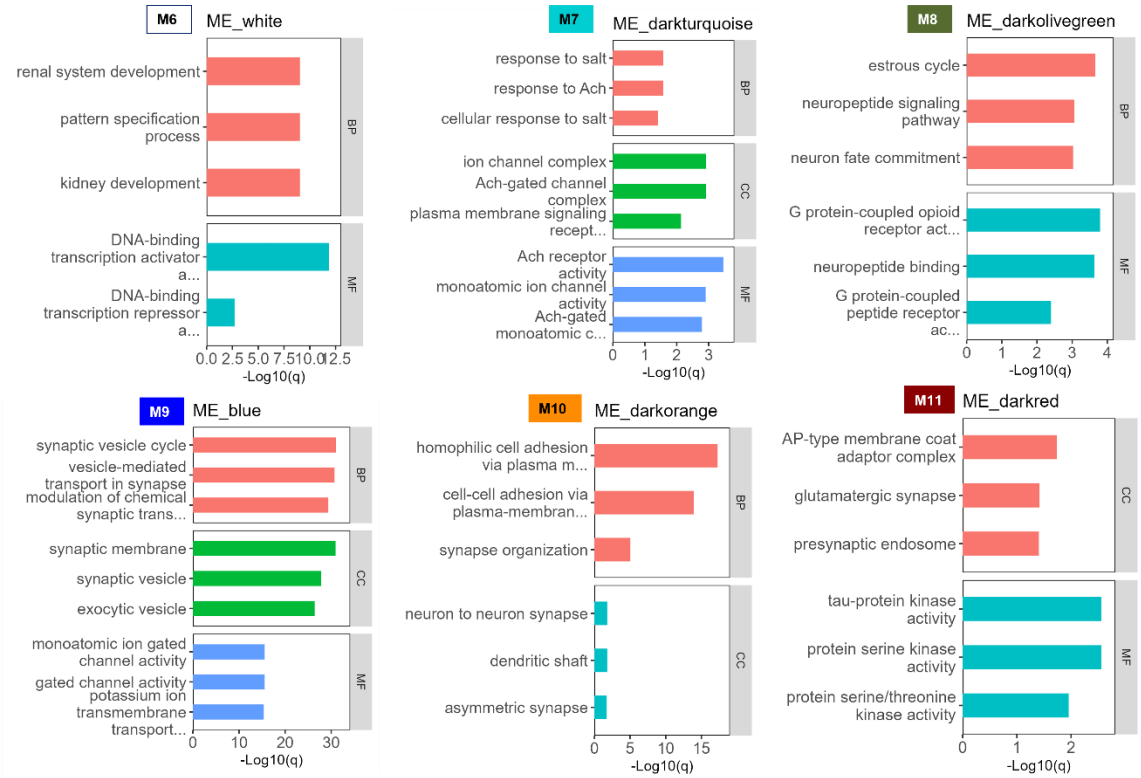

Supplementary Figure 13. Functional annotation of M6-M11 co-expression module genes.

GO enrichment analysis of co-expressed genes in M6-M11 highlighted distinct BP, CC, and MF implicated in neuropsychiatric disorders. For each module, the top three significantly enriched GO terms in each category are shown (*q* value < 0.05).

GO, Gene Ontology; ME, module eigengene; BP, Biological Processes; CC, Cellular Components; MF, Molecular Functions.

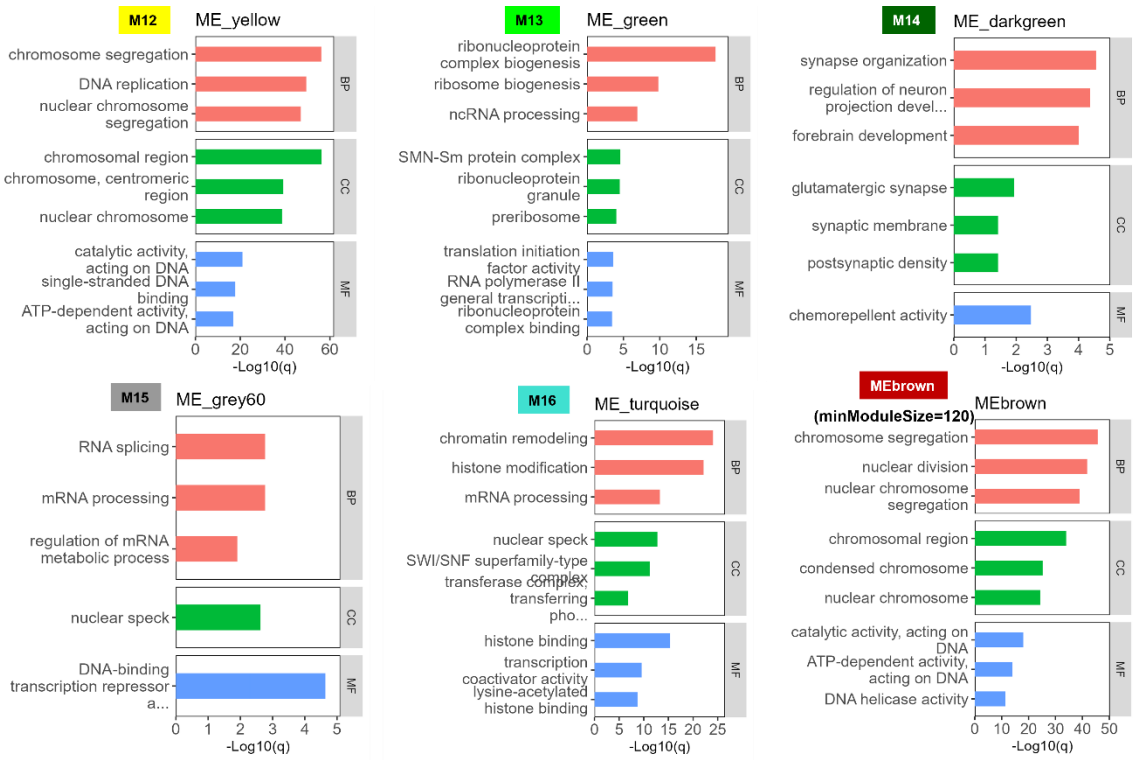

Supplementary Figure 14. Functional annotation of co-expression module M12-M16. GO enrichment analysis of co-expressed genes in M12-M16 revealed distinct BP, CC, and MF implicated in neuropsychiatric disorders. For each module, the top three significantly enriched GO terms in each category are shown (*q* value < 0.05); Notably, an additional module identified when the minimum module size was increased to 120 (ME brown) exhibited highly consistent GO enrichment patterns with module M12 derived using a minimum module size of 40, supporting the robustness of the WGCNA in our analysis with different minimum module size.

GO, Gene Ontology; ME, module eigengene; BP, Biological Processes; CC, Cellular Components; MF, Molecular Functions.

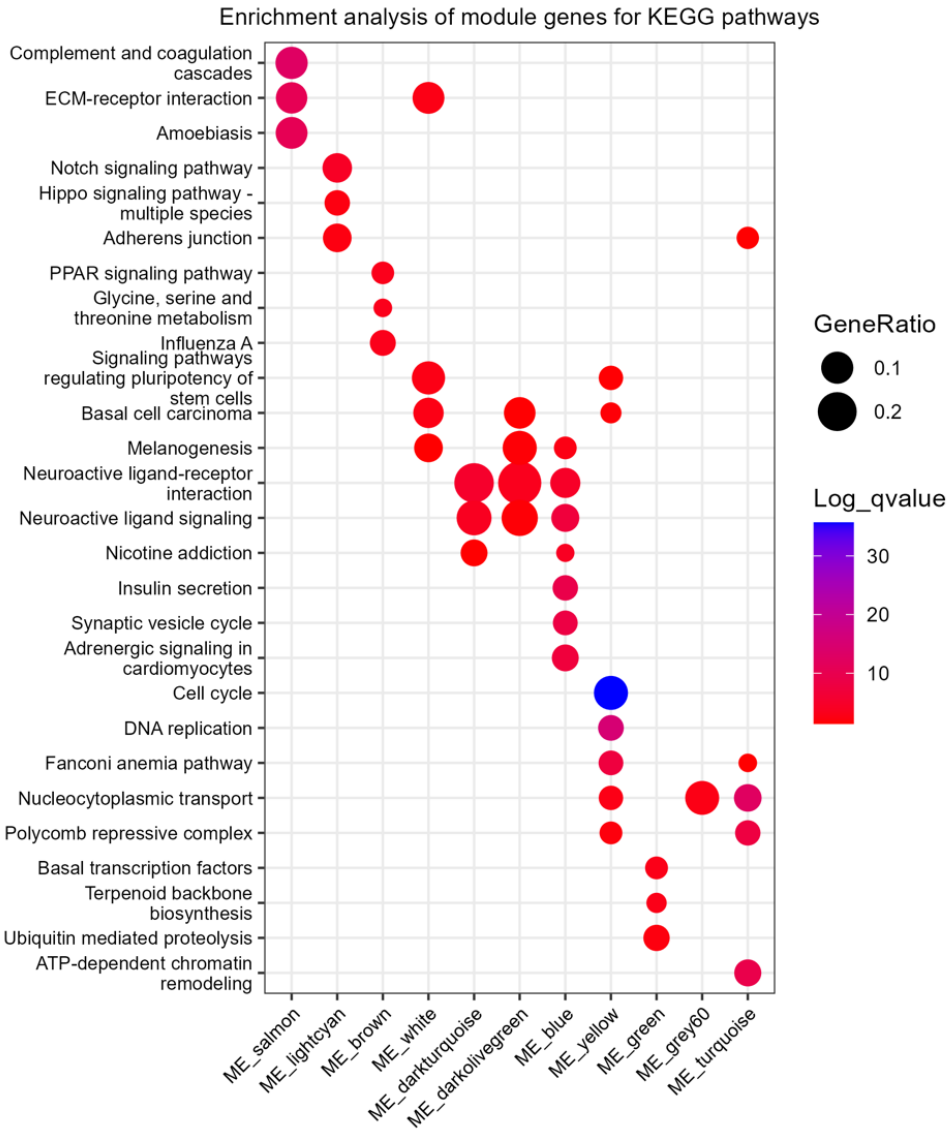

Supplementary Figure 15. KEGG pathway enrichment analysis of genes in the 16 disorder-related co-expression modules.

KEGG pathway enrichment analysis was performed for genes in each of the 16 co-expression modules most significantly associated with neuropsychiatric disorders. The results are displayed as a bubble plot, where each bubble represents a significantly enriched KEGG pathway. The x-axis corresponds to the module ID, and the y-axis indicates the pathway name. Bubble color represents the $-\log_{10}$-transformed *q*-value, indicating the statistical significance of enrichment. Bubble size reflects the gene ratio. Only the top 3 significantly enriched pathways per module are shown. Enriched pathways reflect diverse biological processes in accordance with the corresponding GO items for each module, with the most significant pathway found was “cell cycle” for ME yellow (M12), which was associated with Neuroticism risks.

ME, module eigengene; KEGG, Kyoto Encyclopedia of Genes and Genomes.

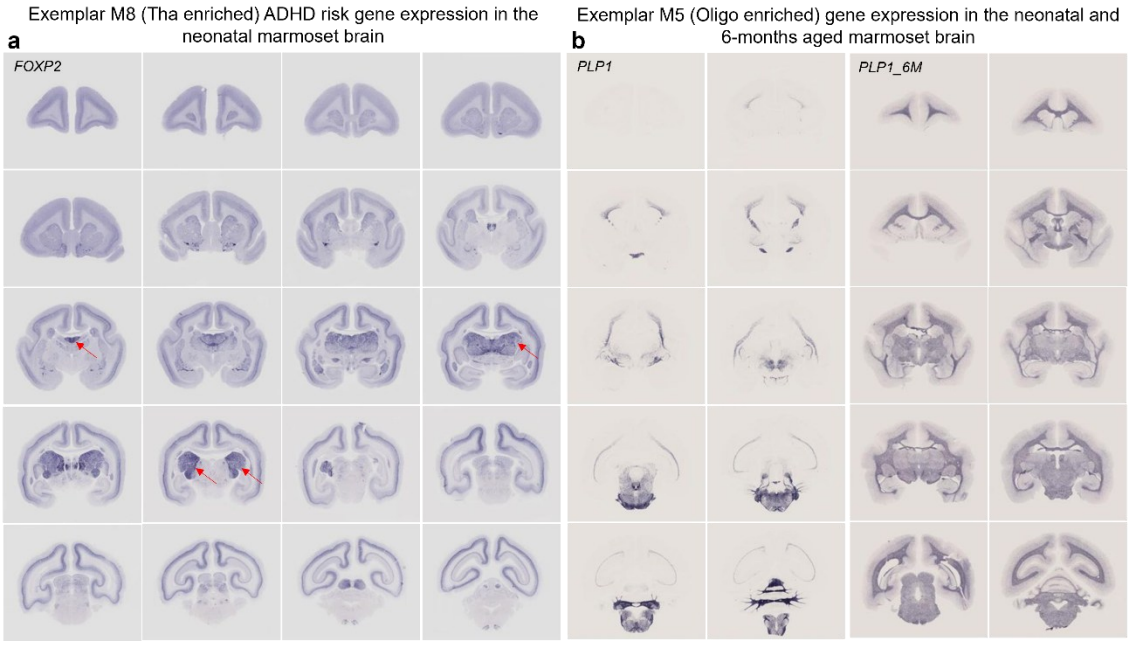

Supplementary Figure 16. Exemplar module-specific risk gene expression across the neonatal marmoset brain.

In situ hybridization (ISH) data from the neonatal marmoset brain were used to examine the whole-brain spatial expression patterns of representative risk genes from co-expression modules enriched for neuropsychiatric risk. (a) Representative M8 module gene (*FOXP2*), associated with ADHD and enriched in the thalamus, shows marked expression in the thalamic region of the neonatal marmoset brain. As indicated by red arrows, *FOXP2* exhibits strong expression in the thalamus, consistent with the spatiotemporal expression pattern of M8 shown in Fig. 6. (b) Representative M5 module gene (*PLP1*), overexpressed in the thalamus and striatum after adolescence and preferentially in the oligodendrocytes (Fig. 6), shows distinct expression in the white matters in neonatal marmoset brain, which was upregulated and extended to the thalamus and striatum at 6 months ages.

ADHD, Attention Deficit Hyperactive Disorder; Oligo, Oligodendrocytes.

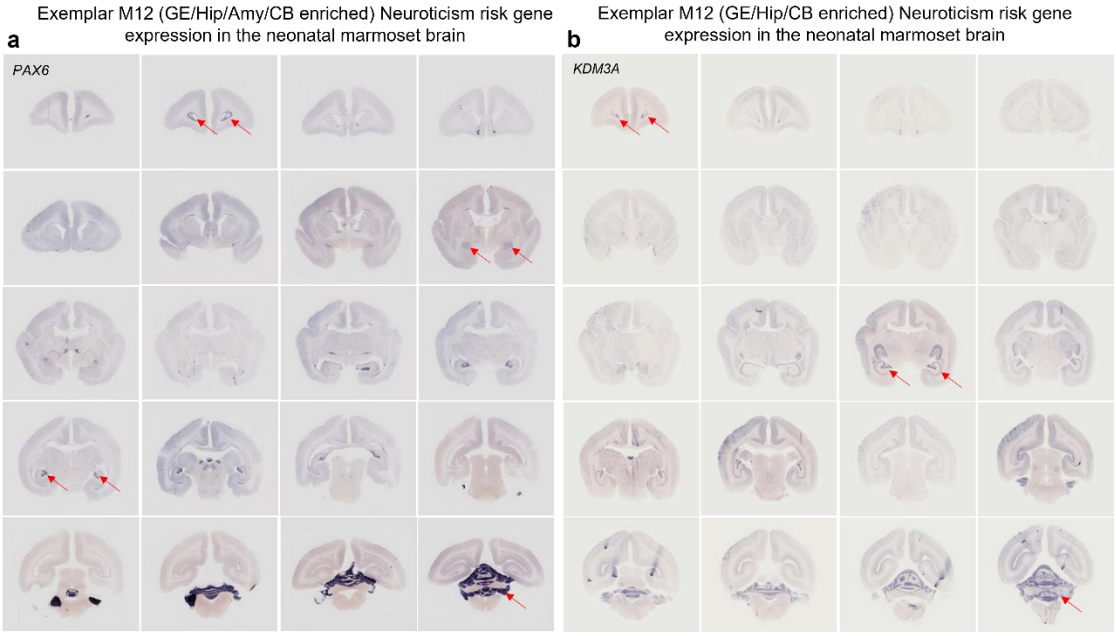

Supplementary Figure 17. Exemplar M12 Neuroticism risk gene expression across the neonatal marmoset brain.

In situ hybridization (ISH) data from the neonatal marmoset brain were used to evaluate the whole-brain spatial expression patterns of representative risk genes from co-expression module M12, which is enriched in the ganglionic eminence (GE), hippocampus (Hip), amygdala (Amy), and cerebellum (CB). (a) Representative M12 neuroticism risk gene *PAX6* exhibits prominent expression in the ventricular zone, central amygdaloid nucleus, dentate gyrus, and cerebellum, as indicated by red arrows, consistent with the spatiotemporal expression pattern of M12 shown in Fig. 6. (b) Representative M12 neuroticism risk gene *KDM3A* shows marked expression in the ventricular zone, hippocampus, and cerebellum, also supporting the M12 module's spatial expression pattern.

GE, Ganglionic Eminence; Amy, Amygdala; Hip, Hippocampus; CB, Cerebellum.

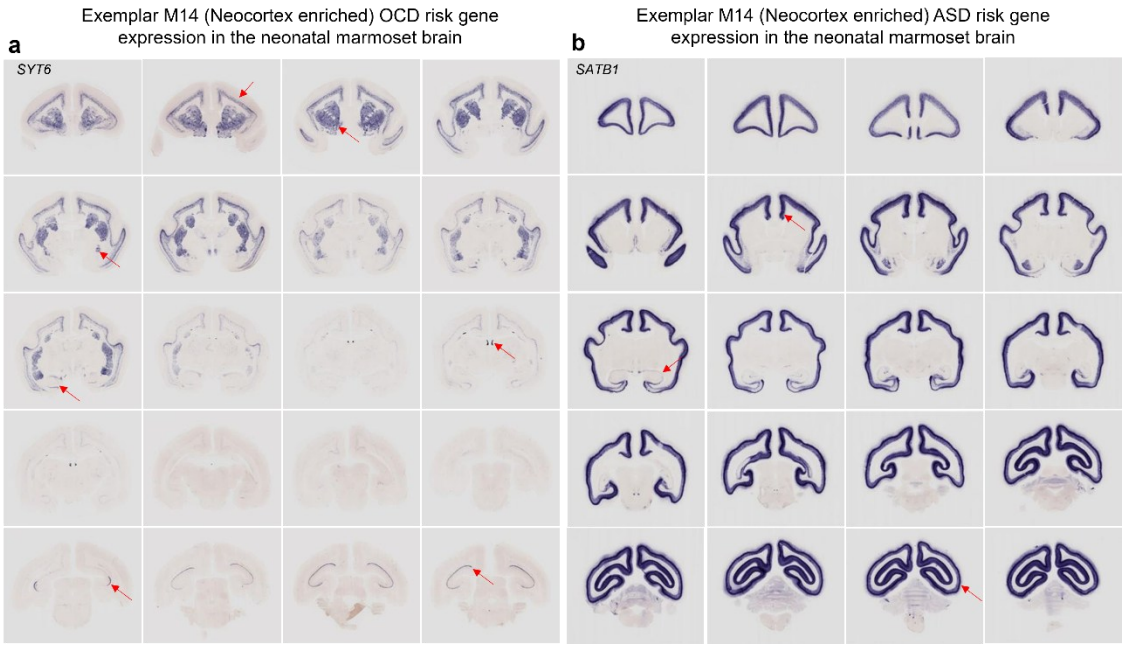

Supplementary Figure 18. Exemplar M14 OCD and ASD risk gene expression across the neonatal marmoset brain.

ISH data from the neonatal marmoset brain were used to examine the spatial expression of representative neuropsychiatric risk genes from co-expression module M14, which is enriched in the neocortex. (a) Representative M14 OCD risk gene *SYT6* exhibits strong expression in the deep layers of the neocortex (specifically in V1 of the occipital cortex), as well as in the striatum, with weaker expression observed in the hippocampus and central amygdaloid nucleus. These patterns are consistent with the spatiotemporal expression profile of M14 shown in Fig. 6. (b) Representative M14 ASD risk gene *SATB1* shows prominent expression in the neocortex and weaker expression in the hippocampus, in accordance with the spatial distribution pattern of M14.

ASD, Autism Spectrum Disorders; OCD, Obsessive Compulsive Disorder.

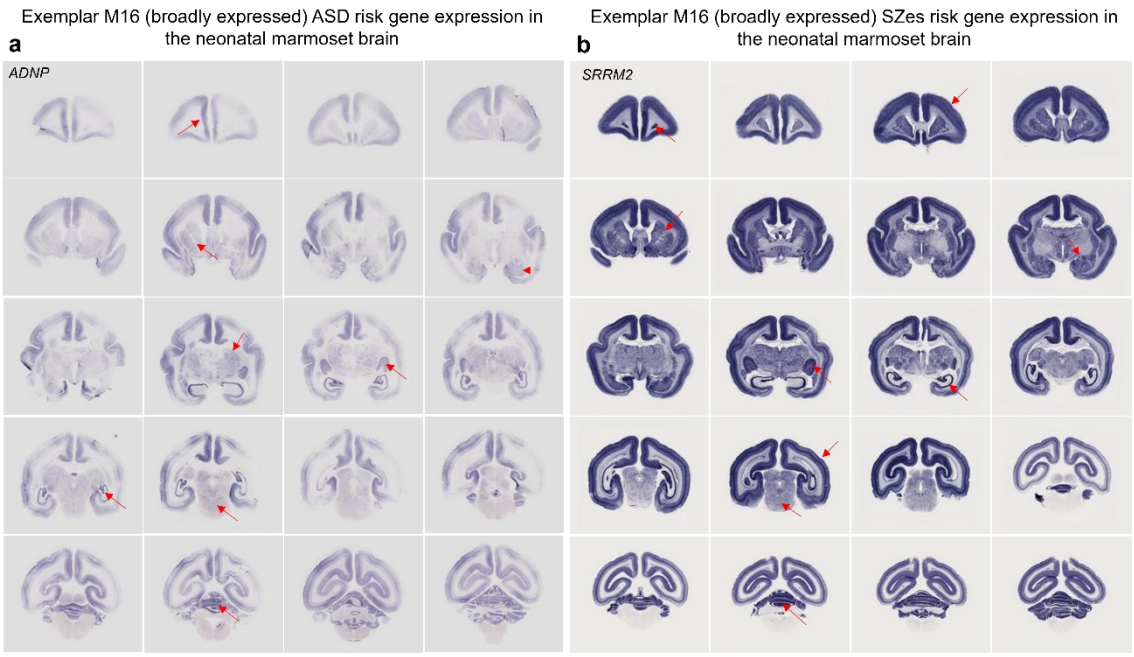

Supplementary Figure 19. Exemplar M16 ASD and SZes risk gene expression across the neonatal marmoset brain.

ISH data from the neonatal marmoset brain were used to examine the spatial expression of representative neuropsychiatric risk genes from co-expression module M16, which is broadly expressed during early neural development. (a) Representative M16 ASD risk gene *ADNP* exhibits widespread expression across the neonatal marmoset brain, consistent with the spatiotemporal expression profile of M16 shown in Fig. 6. (b) Representative M16 SZes risk gene *SRRM2* shows prominent and widespread expression in the neonatal brain, in accordance with the spatial distribution pattern of M16.

ASD, Autism Spectrum Disorders; SZes, Schizophrenia exome sequencing.

Supplementary Table 1. Risk gene sets and their origins used in this study

Risk Gene Datasets	Traits/Control gene sets	Risk Gene Mapping	Num. Risk Genes	Sample Size (case)	Sample Size (total)	Reference
IQ_GWAS_2018 NatGen	Positive Control (early)	MAGMA	507	269,867	269,867	Savage et al., 2018[1]
IQ_GWAS_2018 NatGen_ExNS	Positive Control (early)	ExNS	113	269,867	269,867	Savage et al., 2018[1]
SZ_GWAS_2022 Nature_eQTL_Fetal	Positive Control (early)	eQTL_SMR_Fetal Brain	21	76,755	320,404	Trubetskoy et al., 2022[2]
SZ_GWAS_2022 Nature_eQTL_PEC.adult	Positive Control (late)	eQTL_SMR_PEC Adult Brain	71	76,755	320,404	Trubetskoy et al., 2022[2]
BIP_GWAS_2021NatGen_eQTL_PEC.adult	Positive Control (late)	eQTL_PEC Adult Brain	32	41,917	413,466	Mullins et al., 2021[3]
SZ_High_Confi_Risk_PEC.adult	Positive Control (late)	PEC Regulatory Networks	301	558	1,866	Wang et al., 2018[4]
SZ_Risk_PEC.adult	Positive Control (late)	PEC Regulatory Networks	908	558	1,866	Wang et al., 2018[4]
Random_50	Negative Control	Randomly Selected	50	-	-	-
Random_100	Negative Control	Randomly Selected	100	-	-	-
Random_1000	Negative Control	Randomly Selected	1000	-	-	-
ASD_ES_2020Cell	Autism Spectrum Disorder	Exome Sequencing	102	11,986	35,584	Satterstrom et al., 2020[5]
ASD_ES_2020Cell_Predominant	Autism Spectrum Disorder (Predominant)	Exome Sequencing	53	11,986	35,584	Satterstrom et al., 2020[5]
ASD_ES_2020Cell_NDD	Autism Spectrum Disorder (NDD)	Exome Sequencing	49	11,986	35,584	Satterstrom et al., 2020[5]
ASD_GWAS_2019_Nat_Genet	Autism Spectrum Disorder	MAGMA	25	18,381	46,350	Grove et al., 2019[6]

ASD_SFARI_1	Autism Spectrum Disorder	SFARI "High Confidence"	233	-	-	https://gene.sfari.org/
TS_GWAS_2019AJP	Tourette's Syndrome	Positional	187	4,819	14,307	Yu et al., 2019[7]
Neuroticism_GWAS_2018NatGen	Neuroticism	FUMA/MAGMA	599	449,484	449,484	Nagel et al., 2018[8]
ADHD_GWAS_2019NatGen	Attention Deficit Hyperactive Disorder	Positional	26	19,099	53,293	Demontis et al., 2019[9]
OCD_GWAS_2018MP	Obsessive Compulsive Disorder	Positional	66	2,688	9,725	IOCDF-GC et al., 2018[10]
ANO_GWAS_2019NatGen	Anorexia Nervosa	MAGMA	76	16,992	72,517	Watson et al., 2019[11]
PanicDisorder_GWAS_2019MP	Panic Disorder	MAGMA	41	2,248	10,240	Forstner et al., 2019[12]
BIP_GWAS_2019NatGen	Bipolar Disorder	MAGMA	153	20,352	31,358	Stahl et al., 2019[13]
BIP_GWAS_2021NatGen	Bipolar Disorder	MAGMA	161	41,917	371,549	Mullins et al., 2021[3]
MDD_GWAS_2019NatNeu	Major Depressive Disorder	MAGMA	269	246,363	807,553	Howard et al., 2019[14]
MDD_GWAS_2024NatGen	Major Depressive Disorder	Prioritised (FUMA, MAGMA, Hi-C,TWAS)	964	88,316	991,073	Meng et al., 2024[15]
SZ_ES_2022Nature	Schizophrenia (exome sequencing)	Exome Sequencing	32	24,248	121,570	Singh et al., 2022[16]
SZ_GWAS_2018NatGen_CLZ	Schizophrenia (gwas)	Positional	475	11,260	35,802	Pardinas et al., 2018[17]
SZ_GWAS_2018NatGen_PGC	Schizophrenia (gwas)	Positional	348	11,260	35,802	Pardinas et al., 2018[17]
SZ_GWAS_2022Nature_Ext	Schizophrenia (gwas)	Extended GWAS	638	76,755	320,404	Trubetskoy et al., 2022[2]
SZ_GWAS_2022Nature_Prot	Schizophrenia (gwas)	Portein Coding	437	76,755	320,404	Trubetskoy et al., 2022[2]
SZ_GWAS_2022Nature_Prio	Schizophrenia (gwas)	Prioritized	120	76,755	320,404	Trubetskoy et al., 2022[2]

SZ_GWAS_2022 Nature_FM	Schizophrenia (gwas)	FINEMAP	70	76,755	320,404	Trubetskoy et al., 2022[2]
Epilepsy_GWAS _2018NatCom	Epilepsy	FUMA	146	15,212	44,889	Epilepsy Consortium, 2018[18]
Epilepsy_Monog enic_2018NatCo m	Epilepsy	Selected Monogenic	102	15,212	44,889	Epilepsy Consortium, 2018[18]
Epilepsy_GWAS _2018NatCom_p rio	Epilepsy	Prioritized	38	15,212	44,889	Epilepsy Consortium, 2018[18]
AD_GWAS_202 1NatGen	Alzheimer's Disease	FUMA	978	90,338	226,563	Wightman et al., 2021[19]
AD_GWAS_201 9NatGen	Alzheimer's Disease	Positional/e QTL	192	21,982	63,926	Kunkle et al., 2019[20]
PD_GWAS_201 9LancetNeu	Parkinson's Disease	Positional	97	37.7K	18.6K	Nalls et al., 2019[21]
PD_GWAS_201 9LancetNeu_QT L	Parkinson's Disease	QTL Nominated	62	37.7K	18.6K	Nalls et al., 2019[21]
ADHD_GWAS_2 023NatGen	Attention Deficit Hyperactive Disorder (current)	FUMA	76	38,691	225,534	Demontis et al., 2023[22]
BIP_GWAS_202 5NatNeu	Bipolar Disorder (current)	Positional	924	41917	413466	Koromina et al., 2025[23]
OCD_GWAS_20 25NatGen	Obsessive Compulsive Disorder (current)	multiple gene-based approach	251	53,660	2,098,0 77	Strom et al., 2025[24]
AD_WGS_2025 NatCom	Alzheimer's Disease (current)	LOOCV	2,052	904	1,559	Kim et al., 2025[25]
PD_GWAS_202 3NatGen	Parkinson's Disease (current)	MR-MEGA	133	67,834	2,525,8 97	Kim et al., 2023[26]

GWAS: Genome-Wide Association Studies
ES: Exome Sequencing
AJP: American Journal of Psychiatry
ExNS: Exonic non-synonymous variants;
MAGMA: Multi-marker Analysis of GenoMic Annotation
FUMA: Functional Mapping and Annotation
eQTL: expression Quantitative Trait Loci
SMR: Summary-based Mendelian Randomization
PEC: PsychEnCode
NDD: Neurodevelopmental disorders
MP: Molecular Psychiatry
NatNeu: Nature Neuroscience
NatGen: Nature Genetics
PGC: Psychiatric Genomics Consortium
CLOZUK: Clozapine-treated schizophrenia cohort from the United Kingdom
Ext: Extended GWAS
Prot: Portein Coding
Prio: Prioritized
FM: Fine mapping
T-SEM: Transcriptome-Wide Structural Equation Modeling
LOOCV: leave-one-out cross-validation
MR-MEGA: Meta-Regression of Multi-Ethnic Genetic Association
IQ: Intelligence Quotient
ASD: Autism Spectrum Disorders
ADHD: Attention Deficit Hyperactive Disorder
TS: Tourette's Syndrome
OCD: Obsessive Compulsive Disorder
ANO: Anorexia Nervosa
MDD: Major Depressive Disorder
BIP: Bipolar Disorder
SZes: Schizophrenia exome sequencing:
SZgw: Schizophrenia gwas
AD: Alzheimer's Disease
PD: Parkinson's Disease.

Supplementary References

1. Savage JE, Jansen PR, Stringer S, Watanabe K, Bryois J, de Leeuw CA, Nagel M, Awasthi S, Barr PB, Coleman JRI *et al*: **Genome-wide association meta-analysis in 269,867 individuals identifies new genetic and functional links to intelligence**. *Nat Genet* 2018, **50**(7):912-919.
2. Trubetskoy V, Pardiñas AF, Qi T, Panagiotaropoulou G, Awasthi S, Bigdeli TB, Bryois J, Chen C-Y, Dennison CA, Hall LS *et al*: **Mapping genomic loci implicates genes and synaptic biology in schizophrenia**. *Nature* 2022, **604**(7906):502-508.
3. Mullins N, Forstner AJ, O'Connell KS, Coombes B, Coleman JRI, Qiao Z, Als TD, Bigdeli TB, Borte S, Bryois J *et al*: **Genome-wide association study of more than 40,000 bipolar disorder cases provides new insights into the underlying biology**. *Nat Genet* 2021, **53**(6):817-829.
4. Wang D, Liu S, Warrell J, Won H, Shi X, Navarro FCP, Clarke D, Gu M, Emani P, Yang YT *et al*: **Comprehensive functional genomic resource and integrative model for the human brain**. *Science* 2018, **362**(6420).
5. Satterstrom FK, Kosmicki JA, Wang J, Breen MS, De Rubeis S, An JY, Peng M, Collins R, Grove J, Klei L *et al*: **Large-Scale Exome Sequencing Study Implicates Both Developmental and Functional Changes in the Neurobiology of Autism**. *Cell* 2020, **180**(3):568-584 e523.
6. Grove J, Ripke S, Als TD, Mattheisen M, Walters RK, Won H, Pallesen J, Agerbo E, Andreassen OA, Anney R *et al*: **Identification of common genetic risk variants for autism spectrum disorder**. *Nat Genet* 2019, **51**(3):431-444.
7. Yu D, Sul JH, Tsetsos F, Nawaz MS, Huang AY, Zelaya I, Illmann C, Osiecki L, Darrow SM, Hirschtritt ME *et al*: **Interrogating the Genetic Determinants of Tourette's Syndrome and Other Tic Disorders Through Genome-Wide Association Studies**. *Am J Psychiatry* 2019, **176**(3):217-227.
8. Nagel M, Jansen PR, Stringer S, Watanabe K, de Leeuw CA, Bryois J, Savage JE, Hammerschlag AR, Skene NG, Munoz-Manchado AB *et al*: **Meta-analysis of genome-wide association studies for neuroticism in 449,484 individuals identifies novel genetic loci and pathways**. *Nat Genet* 2018, **50**(7):920-927.
9. Demontis D, Walters RK, Martin J, Mattheisen M, Als TD, Agerbo E, Baldursson G, Belliveau R, Bybjerg-Grauholm J, Baekvad-Hansen M *et al*: **Discovery of the first genome-wide significant risk loci for attention deficit/hyperactivity disorder**. *Nat Genet* 2019, **51**(1):63-75.
10. International Obsessive Compulsive Disorder Foundation Genetics C, Studies OCDCGA: **Revealing the complex genetic architecture of obsessive-compulsive disorder using meta-analysis**. *Mol Psychiatry* 2018, **23**(5):1181-1188.
11. Watson HJ, Yilmaz Z, Thornton LM, Hubel C, Coleman JRI, Gaspar HA, Bryois J, Hinney A, Leppa VM, Mattheisen M *et al*: **Genome-wide association study identifies eight risk loci and implicates metabo-psychiatric origins for anorexia nervosa**. *Nat Genet* 2019, **51**(8):1207-1214.
12. Forstner AJ, Awasthi S, Wolf C, Maron E, Erhardt A, Czamara D, Eriksson E, Lavebratt C, Allgulander C, Friedrich N *et al*: **Genome-wide association study of panic disorder**

reveals genetic overlap with neuroticism and depression. *Mol Psychiatry* 2021, **26**(8):4179-4190.

13. Stahl EA, Breen G, Forstner AJ, McQuillin A, Ripke S, Trubetskoy V, Mattheisen M, Wang Y, Coleman JRI, Gaspar HA *et al*: **Genome-wide association study identifies 30 loci associated with bipolar disorder**. *Nat Genet* 2019, **51**(5):793-803.
14. Howard DM, Adams MJ, Clarke TK, Hafferty JD, Gibson J, Shirali M, Coleman JRI, Hagenaars SP, Ward J, Wigmore EM *et al*: **Genome-wide meta-analysis of depression identifies 102 independent variants and highlights the importance of the prefrontal brain regions**. *Nat Neurosci* 2019, **22**(3):343-352.
15. Meng X, Navoly G, Giannakopoulou O, Levey DF, Koller D, Pathak GA, Koen N, Lin K, Adams MJ, Renteria ME *et al*: **Multi-ancestry genome-wide association study of major depression aids locus discovery, fine mapping, gene prioritization and causal inference**. *Nat Genet* 2024, **56**(2):222-233.
16. Singh T, Poterba T, Curtis D, Akil H, Al Eissa M, Barchas JD, Bass N, Bigdeli TB, Breen G, Bromet EJ *et al*: **Rare coding variants in ten genes confer substantial risk for schizophrenia**. *Nature* 2022, **604**(7906):509-516.
17. Pardinas AF, Holmans P, Pocklington AJ, Escott-Price V, Ripke S, Carrera N, Legge SE, Bishop S, Cameron D, Hamshere ML *et al*: **Common schizophrenia alleles are enriched in mutation-intolerant genes and in regions under strong background selection**. *Nat Genet* 2018, **50**(3):381-389.
18. International League Against Epilepsy Consortium on Complex E: **Genome-wide mega-analysis identifies 16 loci and highlights diverse biological mechanisms in the common epilepsies**. *Nat Commun* 2018, **9**(1):5269.
19. Wightman DP, Jansen IE, Savage JE, Shadrin AA, Bahrami S, Holland D, Rongve A, Borte S, Winsvold BS, Drange OK *et al*: **A genome-wide association study with 1,126,563 individuals identifies new risk loci for Alzheimer's disease**. *Nat Genet* 2021, **53**(9):1276-1282.
20. Kunkle BW, Grenier-Boley B, Sims R, Bis JC, Damotte V, Naj AC, Boland A, Vronskaya M, van der Lee SJ, Amlie-Wolf A *et al*: **Genetic meta-analysis of diagnosed Alzheimer's disease identifies new risk loci and implicates Abeta, tau, immunity and lipid processing**. *Nat Genet* 2019, **51**(3):414-430.
21. Nalls MA, Blauwendraat C, Vallerga CL, Heilbron K, Bandres-Ciga S, Chang D, Tan M, Kia DA, Noyce AJ, Xue A *et al*: **Identification of novel risk loci, causal insights, and heritable risk for Parkinson's disease: a meta-analysis of genome-wide association studies**. *The Lancet Neurology* 2019, **18**(12):1091-1102.
22. Demontis D, Walters GB, Athanasiadis G, Walters R, Therrien K, Nielsen TT, Farajzadeh L, Voloudakis G, Bendl J, Zeng B *et al*: **Genome-wide analyses of ADHD identify 27 risk loci, refine the genetic architecture and implicate several cognitive domains**. *Nature Genetics* 2023, **55**(2):198-208.
23. Koromina M, Ravi A, Panagiotaropoulou G, Schilder BM, Humphrey J, Braun A, Bigdeli T, Chatzinakos C, Coombes BJ, Kim J *et al*: **Fine-mapping genomic loci refines bipolar disorder risk genes**. *Nat Neurosci* 2025, **28**(7):1393-1403.
24. Strom NI, Gerring ZF, Galimberti M, Yu D, Halvorsen MW, Abdellaoui A, Rodriguez-Fontenla C, Sealock JM, Bigdeli T, Coleman JR *et al*: **Genome-wide analyses identify 30**

loci associated with obsessive–compulsive disorder. *Nature Genetics* 2025, **57**(6):1389-1401.

25. Kim JP, Cho M, Kim C, Lee H, Jang B, Jung S-H, Kim Y, Koh IG, Kim S, Shin D *et al*: **Whole-genome sequencing analyses suggest novel genetic factors associated with Alzheimer's disease and a cumulative effects model for risk liability**. *Nature Communications* 2025, **16**(1).

26. Kim JJ, Vitale D, Otani DV, Lian MM, Heilbron K, andMe Research T, Iwaki H, Lake J, Solsberg CW, Leonard H *et al*: **Multi-ancestry genome-wide association meta-analysis of Parkinson's disease**. *Nat Genet* 2024, **56**(1):27-36.